International Advance Journal of Engineering Research (IAJER)
*Volume 09, Issue 06 (**June - 2026**), PP 01-12*
ISSN: 2360-819X
www.iajer.com

Research Paper **Open Access**

GEOTECHNICAL RESPONSE OF FINE- AND COARSE-GRAINED SOILS TO COMBINED DIESEL AND WASTE ENGINE OIL CONTAMINATION

J. E. Agori[1]*, L. U. Umukoro[1], S. U. Okoroafor[2], J. Oba[1], E. Obayehagweme[3], and C. L. Opone[1]

[1]*Department of Civil Engineering, Delta State University, Abraka, Nigeria Faculty of Engineering, Oleh Campus, P. M. B. 22, Oleh.
[2]Department of Civil Engineering, Michael Okpara University of Agriculture, Umudike.
[3]Department of Civil Engineering, Federal Polytechnic, Orogun, Delta State.

ABSTRACT: Fine- and coarse-grained soils at waste-handling, fuelling, and industrial spill sites are frequently exposed to petroleum hydrocarbons from diesel and waste engine oil. Despite shared petroleum origins, these contaminants differ substantially in composition, volatility, viscosity, and chemical reactivity, which can lead to complex and time-dependent changes in soil behaviour. At the field scale, the effects of combined diesel and waste engine oil contamination may not be predictable from data developed for single contaminants, particularly when soils vary widely in grain size distribution, mineralogy, and fabric. Current geotechnical assessment practices often rely on simplified assumptions about contaminant loading and soil response, leaving key gaps in understanding the coupled mechanisms driving changes in engineering properties. These mechanisms can vary between fine-grained soils (e.g., via pore structure and adsorption effects) and coarse-grained soils. Therefore, there is a need to develop a scientifically grounded understanding of how combined diesel and waste engine oil contamination impacts the geotechnical response of fine- and coarse-grained soils across relevant contamination concentrations and exposure durations. This study evaluated the combined effect of diesel and waste engine oil on the geotechnical properties of both fine-grained (clay) and coarse-grained (sand) soils. A controlled laboratory experiment was performed by contaminating soil samples with a standardized petroleum product mixture (80% diesel, 20% waste engine oil) at varying concentrations (0% to 16% by weight). Key geotechnical parameters, including Atterberg limits, compaction characteristics, shear strength, California Bearing Ratio (CBR), and permeability, were determined in accordance with ASTM and BS standards. A two-way ANOVA was employed to analyse the influence of soil type, contamination level, and their interaction. The results demonstrated that combined contamination significantly degraded the engineering properties of both soil types, with fine-grained soils exhibiting greater sensitivity. The principal findings revealed a decrease in maximum dry density (MDD) of up to 16.9% in fine-grained soil and 13.5% in coarse-grained soil, coupled with a severe reduction in soaked CBR by 26.5% and 38.6%, respectively. The angle of internal friction declined markedly, while permeability decreased in both soils due to pore clogging by hydrocarbons. The study concludes that even low levels of mixed hydrocarbon contamination can render both fine- and coarse-grained soils unsuitable for structural applications without prior remediation or stabilization, highlighting a critical consideration for geotechnical practice in contaminated environments.

Keywords: Combined petroleum contamination, Diesel, Waste engine oil, Fine-grained soil, Coarse-grained soil, Geotechnical properties

I. Introduction

Soil, a fundamental geomaterial in civil engineering, serves as the foundation for nearly all infrastructure. Its stability, strength, and deformation characteristics are paramount to the safety and longevity of buildings, pavements, and earth structures (Budhu, 2011; Das, 2010). However, the uncontrolled release of petroleum hydrocarbons into the soil presents a formidable challenge, profoundly altering the very properties that make soil a reliable construction material. This issue is particularly acute in regions with intensive oil exploration, transportation, and refining activities, such as the Niger Delta in Nigeria, where accidental spills, pipeline vandalism, and improper disposal of waste lubricants around mechanic workshops are recurrent (Ibrahim et al., 2020; Kadafa, 2012). The infiltration of these hydrocarbons into the soil matrix compromises its load-bearing capacity, setting the stage for structural failures if not adequately addressed.

The geotechnical consequences of soil contamination by individual petroleum products have been the subject of considerable research. Studies have consistently shown that crude oil and its derivatives, such as diesel and engine oil, act as lubricants between soil particles, diminishing inter-particle friction and cohesion, and thereby reducing shear strength (Khamehchiyan et al., 2007; Nwachukwu et al., 2020; Oyegbile & Ayininuola, 2013). Hydrocarbons also influence compaction behavior, generally leading to a reduction in maximum dry density (MDD) and an alteration of optimum moisture content (OMC) (Akinwumi et al., 2014; Al-Sanad et al., 1995). Furthermore, they affect soil consistency by coating clay particles and disrupting the diffuse double layer, typically causing a decrease in Atterberg limits, although some studies have reported increases depending on the specific contaminant and soil mineralogy (Kermani & Ebadi, 2012; Tse & Eshiemomo, 2016). The permeability of contaminated soils is also known to be affected, with fine-grained soils potentially becoming more permeable due to structural disruption, while coarse-grained soils may experience pore clogging, leading to a decrease in hydraulic conductivity (Nwachukwu et al., 2020; Rahman et al., 2010). These collective alterations can severely compromise a soil's suitability as a subgrade or foundation material (George et al., 2014; Oluremi et al., 2017).

A significant knowledge gap persists, however, in understanding the impacts of combined or mixed hydrocarbon pollution. In real-world contamination scenarios, such as those from leaking underground storage tanks at filling stations, mechanic workshops or mixed industrial effluents, soils are rarely exposed to a single type of petroleum product. Diesel and waste engine oil, in particular, frequently co-occur as environmental pollutants due to their widespread use in transportation and heavy machinery. Diesel is a light, less viscous fuel, while waste engine oil is a heavy viscous liquid containing suspended metal particles and other degradation by products (Obeta & Eze-Uzomaka, 2013). The synergistic or antagonistic interaction of these two distinct hydrocarbons within a soil matrix is largely unexplored, leaving engineers without the necessary data to make informed predictions about soil behavior at sites contaminated by a mixture of diesel and waste engine oil.

This study is designed to address this gap by systematically evaluating the combined effect of diesel and waste engine oil contamination on both fine- and coarse-grained soils. A comparative approach is necessary because the inherent properties of these soil classes dictate vastly different baseline geotechnical behaviours and responses to pollutants. Fine-grained soils, with their high specific surface area and complex electro-chemical interactions, are hypothesized to be more susceptible to physio-chemical changes, while coarse-grained soils are expected to be predominantly affected by the physical lubrication of their particle contacts. The primary objective is to quantify the degradation of critical geotechnical parameters, namely Atterberg limits, compaction (MDD and OMC), shear strength (angle of internal friction and cohesion), soaked CBR, and permeability, across a range of contaminant concentrations. A secondary objective is to assess whether the interaction between soil type and contamination level is statistically significant for these properties. By elucidating these combined effects, this research aims to provide a more realistic basis for the geotechnical assessment, remediation, and stabilization of petroleum-polluted sites, ultimately contributing to safer and more sustainable Civil Engineering practices.

II. Materials and Methods

2.1. Study Design

This investigation employed a controlled experimental laboratory design to isolate and quantify the effects of combined diesel and waste engine oil contamination on the geotechnical properties of two distinct soil types. A factorial experimental design was adopted with two independent variables: soil type (fine-grained and coarse-grained) and contamination level (nine levels, including a 0% control and eight contamination percentages). The primary outcomes measured were a suite of geotechnical parameters, and a two-way analysis of variance (ANOVA) was used to determine the significance of the main effects and their interaction. This design was chosen because it allows for a rigorous comparison of how different soils respond to varying proportions of the same pollutant, a scenario relevant to practical conditions where a mixed contaminant plume may encounter stratified soil layers.

2.2. Research Setting and Sample Collection

The study was conducted using soil samples collected from Oleh, Isoko South Local Government Area, Delta State, Nigeria, a region within the Niger Delta basin underlain by sedimentary formations including alluvial and deltaic deposits. To ensure a clear contrast in soil properties, the two soil types were sourced from distinct locations. The fine-grained (cohesive) soil was obtained from a flood basin with poor drainage, yielding a soil high in clay content. The coarse-grained (granular) soil was collected from the bed of the River Niger, providing a clean, predominantly sandy soil. Disturbed soil samples were collected at depths of 0.5 m to 1.5 m below ground level using a hand auger to avoid the organic-rich topsoil, following standard practice for geotechnical and environmental sampling (Ahmadi et al., 2021). The samples were air-dried and stored in airtight containers prior to initial characterization and subsequent contamination. The contaminants, diesel and

waste vehicle oil, were sourced locally from a Rain Oil filling station and a mechanic workshop, both in Oleh, Delta State.

2.3. Materials Characterization and Contamination Procedure

The diesel and waste engine oil were combined to create a uniform contaminant mixture, designated as Petroleum Product 2 (PP2), comprising 80% diesel and 20% waste engine oil by volume. This ratio was selected to simulate a common field scenario where a larger fraction of light fuel oil is mixed with a heavier, more viscous lubricant.

The uncontaminated fine-grained and coarse-grained soils were first characterized for their baseline geotechnical properties. A sixteen-sample experimental plan was established for each soil type, consisting of a control (uncontaminated) and eight contamination levels (SAM 1 to SAM 8). The PP2 mixture was thoroughly blended with the soils at concentrations of 2%, 4%, 6%, 8%, 10%, 12%, 14%, and 16% by dry weight of the soil. The contaminated soil samples were then sealed in airtight containers and allowed to acclimatize for 28 days, a period intended to permit a thorough interaction and chemical equilibrium between the hydrocarbon mixture, soil particles, and any pore water present (Ijimdiya, 2013).

2.4. Laboratory Testing Program

A comprehensive suite of geotechnical laboratory tests was conducted on both the uncontaminated (control) and contaminated soil samples, strictly following recognized international standards. The tests were performed to determine index properties, compaction characteristics, strength, bearing capacity, and hydraulic conductivity.

Particle size distribution was determined through sieve analysis for the coarse-grained soil and a combined sieve and hydrometer analysis for the fine-grained soil (ASTM D422). Specific gravity was determined using the density bottle method (ASTM D854). Consistency limits, including liquid limit (LL) and plastic limit (PL), were measured using the Casagrande apparatus and the manual rolling method respectively, according to ASTM D4318. The plasticity index (PI) was calculated as the difference between LL and PL. The free swelling index (FSI) was measured by comparing the settled volume of oven-dried soil in distilled water and kerosene in a graduated cylinder (ASTM D720/D720M).

Compaction characteristics were evaluated using the Standard Proctor test (ASTM D698). The soil was compacted in a 1-liter mould in three layers, with each layer receiving 25 blows from a 2.6 kg rammer dropped from a height of 30 cm. Maximum Dry Density (MDD) and Optimum Moisture Content (OMC) were derived from the compaction curve. Direct shear tests were performed to determine shear strength parameters on samples compacted at their respective MDD and OMC (ASTM D3080). The tests were run on a 100 mm × 100 mm shear box at three different normal stresses (50, 100, and 200 kPa) with a shearing rate of 1 mm/min. The cohesion (c) and angle of internal friction (φ) were determined from the Mohr-Coulomb failure envelope.

The California Bearing Ratio (CBR) was determined for samples compacted at their optimum condition using the Standard Proctor effort (ASTM D1883). These specimens were soaked in water for 96 hours to simulate a worst-case field condition before penetration testing. The penetration resistance of a 50 mm diameter plunger at a rate of 1.25 mm/min was recorded, and the CBR values at 2.5 mm and 5.0 mm penetration were calculated. The falling head permeability test was conducted on compacted specimens in a rigid-wall permeameter cell (ASTM D5084). The coefficient of permeability (k) was calculated by measuring the time interval required for a head to drop between two reference points on a standpipe.

A two-way analysis of variance (ANOVA) was used to statistically evaluate the effects of soil type, contamination level, and their interaction on the measured geotechnical properties at a 5% significance level ($p \leq 0.05$).

III. Results and Discussion

3.1 Geotechnical Properties of Uncontaminated Soils

The baseline geotechnical properties of the two soils, prior to any contamination, are summarised in Table 1. The characterisation confirmed the selection of two fundamentally different soil types. The fine-grained soil, with 33.2% fines, exhibited properties typical of a clay of intermediate plasticity, while the coarse-grained soil, containing only 1.2% fines, behaved as a clean, non-plastic sand. The particle size distribution curves for both soils are presented in Figure 1.

The specific gravity of the coarse-grained soil (3.36) was substantially higher than that of the fine-grained soil (2.45), reflecting a mineralogical composition richer in dense minerals such as quartz and feldspar (Yuan et al., 2019). Atterberg limits clearly distinguished the two materials. The fine-grained soil had a liquid limit (LL) of 43.67% and a plastic limit (PL) of 25.33%, resulting in a plasticity index (PI) of 18.33%, indicative of greater water retention capacity and potential for volume change. In contrast, the coarse-grained soil displayed a liquid limit of 27.00% and was non-plastic, confirming its granular nature.

Table 1: Geotechnical Properties of Uncontaminated Soil Samples (Mean ± SD)

Parameter	Fine-grained Soil	Coarse-grained Soil
Specific Gravity	2.45 ± 0.04	3.36 ± 0.09
Liquid Limit (%)	43.67 ± 1.53	27.00 ± 1.41
Plastic Limit (%)	25.33 ± 1.53	N/A
Plasticity Index (%)	18.33 ± 2.31	N/A
Compaction: MDD (g/cm³)	1.36 ± 0.03	1.78 ± 0.06
Compaction: OMC (%)	17.14 ± 0.10	14.40 ± 0.23
Angle of Internal Friction (°)	25.33 ± 0.58	33.67 ± 1.53
Cohesion (kN/m²)	10.91 ± 0.80	0.00
Soaked CBR (%)	2.94 ± 0.08	14.02 ± 0.25
Permeability (m/s)	$2.26 \times 10^{-8} \pm 2.65 \times 10^{-10}$	$1.08 \times 10^{-4} \pm 4.04 \times 10^{-6}$
Free Swelling Index (%)	18.03 ± 0.11	2.03 ± 0.05

Significant contrasts were also observed in mechanical and hydraulic properties. The coarse-grained soil demonstrated superior load-bearing capacity with a soaked California Bearing Ratio (CBR) of 14.02%, compared to only 2.94% for the fine-grained soil, confirming its higher resistance to penetration (Tamassoki et al., 2023). Permeability was four orders of magnitude greater in the coarse-grained soil (1.08×10^{-4} m/s) than in the fine-grained soil (2.26×10^{-8} m/s), a direct consequence of the larger, more interconnected pore spaces in the sand (Nachum, 2025). Compaction characteristics also diverged markedly; the coarse-grained soil achieved a higher maximum dry density (MDD) of 1.78 g/cm³ at a lower optimum moisture content (OMC) of 14.40%, whereas the fine-grained soil reached an MDD of only 1.36 g/cm³ at a higher OMC of 17.14%, illustrating its greater water demand for compaction.

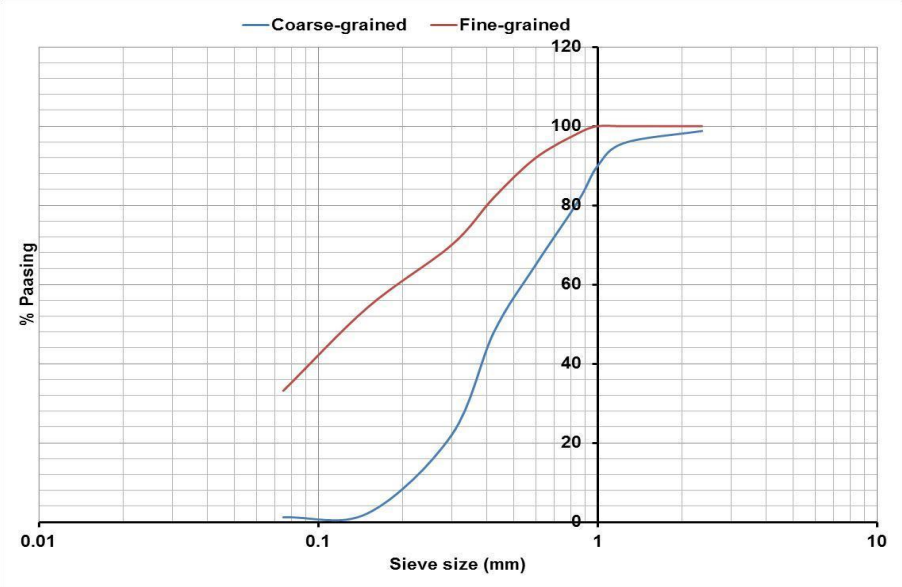

Figure1: Particle Size Distribution Curves for Uncontaminated Soils

The free swelling index was markedly higher in the fine-grained soil (18.03%) than in the coarse-grained soil (2.03%), signalling its expansive nature. Shear strength parameters further underscored the textural differences: the coarse-grained soil was friction-dominated with an angle of internal friction (φ) of 33.67° and zero cohesion, while the fine-grained soil exhibited both frictional (φ = 25.33°) and cohesive (c = 10.91 kN/m²) resistance.

3.2 Atterberg Limits of Contaminated Soils

Atterberg limits describe the changes in the consistency of fine-grained soils in different moisture contents, and they are used to classify and characterize these soils. The effects of the combined diesel and waste engine oil contamination on the consistency limits were statistically evaluated using a two-way ANOVA, the results of which are presented in Table 2. The analysis revealed that soil type, contamination level, and their interaction all had a highly significant effect ($p < 0.05$) on liquid limit (LL), plastic limit (PL), and plasticity index (PI). This confirms that the inherent characteristics of the soil and the contaminant concentration jointly

govern the observed changes in plasticity. The Atterberg Limits and Plasticity Index of the oil contaminated fine-grained soil have shown an increase of about 3-5%.

The mean values for Atterberg limits across all contamination levels are detailed in Table 3. For fine-grained soil, the LL of the control specimen was 43.67%. A notable initial increase was observed at low contamination levels, with LL rising to 48.67% at 4% contaminant concentration (SAM 2). As crude oil content increases, LL values of soil have small changes, while PL increases, and PI decreases. An almost similar pattern was observed by (Araz et al., 2021). However, this trend reversed at higher levels, with LL declining sharply to a minimum of 26.67% at 16% contamination (SAM 8). The plastic limit for this soil followed a similar trend, increasing from 25.33% to a peak of 28.33% at SAM 2 before decreasing progressively to 12.67% at SAM 8. Consequently, the plasticity index peaked at 20.33% at SAM 2 and then declined to a low of 13.33% at SAM 7. In the coarse-grained soil, which was initially non-plastic, apparent plasticity emerged with contamination. The liquid limit increased from 27.00% (control) to a peak of 34.33% at SAM 3 before declining to 22.67% at the highest contamination level. The coarse soil remained non-plastic (PL = 0) throughout, and the reported plasticity index values are therefore a reflection of this apparent, non-standard plastic behavior. The addition of crude oil caused an increase in the Atterberg limits and the plasticity index. The most probable reason for the increase in Atterberg limits is the extra cohesion provided to the clay particles by the oil (Habib-ur-Rehman et al., 2017). Therefore, additional water is required to cause sufficient layer thickness to change soil from one consistency to the other consistency.

Table 2: Two-Way ANOVA Results for the Effect of Contamination on Atterberg Limits

Source	Parameter	Sum of Squares	df	Mean Square	F	p-value
Soil type	LL	1246.288	1	1246.288	660.910	2.59E-24*
	PL	6400.288	1	6400.288	5333.574	7.53E-40*
	PI	1998.000	1	1998.000	647.500	3.65E-24*
Contamination	LL	1255.148	8	156.893	83.201	1.79E-20*
	PL	371.667	8	46.458	38.715	3.76E-15*
	PI	298.481	8	37.310	12.091	4.37E-08*
Soil type × Contamination	LL	516.875	8	64.609	34.263	2.44E-14*
	PL	371.667	8	46.458	38.715	3.76E-15*
	PI	157.542	8	19.693	6.382	4.19E-05*

*Note: * indicates significance at $p \leq 0.05$.*

Table 3: Atterberg Limits of Contaminated Soil Samples (Mean ± SD)

Factor	LL (%) Fine	LL (%) Coarse	PL (%) Fine	PL (%) Coarse	PI (%) Fine	PI (%) Coarse
Control	43.67 ± 1.53	27.00 ± 1.41	25.33 ± 1.53	0.00	18.33 ± 2.31	27.00 ± 1.41
SAM 1 (2%)	46.67 ± 1.53	27.33 ± 1.53	27.67 ± 2.08	0.00	19.00 ± 2.65	27.33 ± 1.53
SAM 2 (4%)	48.67 ± 1.53	30.00 ± 1.00	28.33 ± 0.58	0.00	20.33 ± 1.15	30.00 ± 1.00
SAM 3 (6%)	44.00 ± 1.00	34.33 ± 1.53	26.33 ± 1.53	0.00	17.67 ± 2.31	34.33 ± 1.53
SAM 4 (8%)	39.33 ± 1.53	33.33 ± 1.15	23.33 ± 1.15	0.00	16.00 ± 1.73	33.33 ± 1.15
SAM 5 (10%)	36.00 ± 1.00	30.33 ± 1.53	21.67 ± 1.15	0.00	14.33 ± 1.53	30.33 ± 1.53
SAM 6 (12%)	33.33 ± 1.53	28.67 ± 1.53	17.67 ± 0.58	0.00	15.67 ± 1.53	28.67 ± 1.53
SAM 7 (14%)	29.00 ± 1.00	26.00 ± 1.00	15.67 ± 2.52	0.00	13.33 ± 2.08	26.00 ± 1.00
SAM 8 (16%)	26.67 ± 1.53	22.67 ± 1.53	12.67 ± 1.53	0.00	14.00 ± 2.65	22.67 ± 1.53

3.3 Compaction Characteristics

The ANOVA for compaction parameters (Table 4) demonstrated that both soil type and contamination level had a highly significant effect on MDD and OMC ($p < 0.05$). The interaction effect between soil type and contamination was not significant for MDD ($p = 0.56$), indicating that the contaminant-induced reduction in density followed a similar proportional pattern in both soils. However, the interaction was significant for OMC ($p < 0.05$), confirming that the increase in water demand was soil dependent.

The mean MDD and OMC values under varying contaminant concentrations are shown in Table 5. For both soils, an inverse relationship between MDD and OMC was observed as contamination increased. In fine-grained soil, the MDD decreased progressively from 1.36 g/cm³ (control) to 1.13 g/cm³ at SAM 8, representing a 16.9% reduction. Concurrently, the OMC rose from 17.14% to 19.81%. A similar, though less pronounced,

trend was observed in the coarse-grained soil, where MDD fell from 1.78 g/cm³ to 1.54 g/cm³ (a 13.5% decrease), and OMC increased from 14.40% to 17.88%. The deterioration in compaction efficiency was statistically significant even at the lowest contamination level (2%) for both soil types.

Table 4: Two-Way ANOVA Results for the Effect of Contamination on Compaction Behaviour

Source	Parameter	Sum of Squares	df	Mean Square	F	p-value
Soil type	MDD	2.596	1	2.596	2396.335	1.55E-34*
	OMC	58.907	1	58.907	1712.587	5.89E-32*
Contamination	MDD	0.327	8	0.041	37.753	3.00E-15*
	OMC	52.527	8	6.566	190.888	4.14E-27*
Soil type × Contamination	MDD	0.007	8	0.001	0.858	0.5596
	OMC	2.279	8	0.285	8.282	2.72E-06*

*Note: * indicates significance at p≤ 0.05.*

Table 5: Compaction Characteristics of Contaminated Soil Samples (Mean ± SD)

Factor	MDD Fine (g/cm³)	MDD Coarse (g/cm³)	OMC Fine (%)	OMC Coarse (%)
Control	1.36 ± 0.03	1.78 ± 0.06	17.14 ± 0.10	14.40 ± 0.23
SAM 1 (2%)	1.28 ± 0.03	1.76 ± 0.03	17.45 ± 0.19	14.83 ± 0.43
SAM 2 (4%)	1.27 ± 0.02	1.73 ± 0.02	17.89 ± 0.15	15.32 ± 0.26
SAM 3 (6%)	1.24 ± 0.02	1.69 ± 0.03	18.17 ± 0.09	16.17 ± 0.28
SAM 4 (8%)	1.19 ± 0.02	1.64 ± 0.04	18.47 ± 0.18	16.79 ± 0.19
SAM 5 (10%)	1.17 ± 0.01	1.61 ± 0.03	18.83 ± 0.09	16.95 ± 0.08
SAM 6 (12%)	1.16 ± 0.01	1.58 ± 0.07	18.88 ± 0.19	17.28 ± 0.09
SAM 7 (14%)	1.14 ± 0.01	1.55 ± 0.05	19.27 ± 0.06	17.49 ± 0.06
SAM 8 (16%)	1.13 ± 0.01	1.54 ± 0.04	19.81 ± 0.13	17.88 ± 0.08

3.4 Shear Strength Parameters

The shear strength of soil is a crucial property since it controls bearing capacity as well as stability of the foundation system of a civil engineering structure. The ANOVA results for shear strength parameters (Table 6) confirmed that soil type and contamination level significantly influenced both the angle of internal friction and cohesion ($p < 0.05$). The interaction between soil type and contamination was significant for cohesion but not for the friction angle, indicating that the loss of frictional resistance was similar across both soil types, whereas the change in cohesion was highly dependent on soil type.

The mean shear strength parameters are presented in Table 7. In fine-grained soil, the angle of internal friction (φ) fell consistently from 25.33° (control) to 14.00° at SAM 8, a total reduction of 44.7%. Cohesion (c), however, displayed a contrasting pattern. It increased sharply from 10.91 kN/m² to a peak of 16.15 kN/m² at 2% contamination (SAM 1) before declining steadily to a value equivalent to the original baseline (10.91 kN/m²) at the highest contamination level. For coarse-grained soil, which had no true cohesion, the friction angle decreased from 33.67° to 22.67°, a 32.7% reduction, while cohesion remained at zero across all samples. The samples were compacted at the field dry density of 12 kN/m3. Results indicate that at low confining pressures, the strength of the contaminated soil was less than that of the uncontaminated one, while at high confining pressures; the strength was a little more than that of the uncontaminated one. The increase in the strength of the oil mixed fine-grained soil could be attributed to the agglomeration of particles in the presence of oil (Habib-ur-Rehman et al., 2017).

Table 6: Two-Way ANOVA Results for the Effect of Contamination on Shear Strength

Source	Parameter	Sum of Squares	df	Mean Square	F	p-value
Soil type	φ	979.630	1	979.630	391.85	6.15E-21*
	Cohesion	2564.458	1	2564.458	9247.02	5.21E-45*
Contamination	φ	790.370	8	98.796	39.52	1.46E-15*
	Cohesion	95.627	8	11.953	43.10	3.65E-16*
Soil type × Contamination	φ	9.704	8	1.213	0.49	0.859
	Cohesion	95.627	8	11.953	43.102	3.65E-16*

*Note: * indicates significance at p≤ 0.05.*

Table 7: Shear Strength Parameters of Contaminated Soil Samples (Mean ± SD)

Factor	φ Fine (°)	φ Coarse (°)	c Fine (kN/m²)	c Coarse (kN/m²)
Control	25.33 ± 0.58	33.67 ± 1.53	10.91 ± 0.80	0.00
SAM 1 (2%)	24.00 ± 1.00	33.33 ± 2.08	16.15 ± 1.02	0.00
SAM 2 (4%)	23.00 ± 1.00	32.33 ± 0.58	15.01 ± 0.21	0.00
SAM 3 (6%)	21.00 ± 1.00	30.33 ± 1.15	13.09 ± 0.27	0.00
SAM 4 (8%)	20.33 ± 1.53	28.00 ± 2.65	13.02 ± 0.23	0.00
SAM 5 (10%)	18.67 ± 1.53	26.00 ± 1.00	12.63 ± 0.40	0.00
SAM 6 (12%)	16.67 ± 2.08	24.33 ± 2.52	11.85 ± 0.34	0.00
SAM 7 (14%)	15.33 ± 1.53	23.33 ± 2.08	11.51 ± 0.42	0.00
SAM 8 (16%)	14.00 ± 1.00	22.67 ± 1.53	10.91 ± 0.80	0.00

3.5 Soaked California Bearing Ratio (CBR)

The soaked CBR values for both soils across all contamination levels are illustrated in Figure 2. The coarse-grained control soil had a far higher CBR (14.02%) than the fine-grained control (2.94%). Contamination caused a consistent decline in CBR for both materials. In fine-grained soil, the CBR decreased from 2.94% to 2.16% at SAM 8, a 26.5% reduction. The coarse-grained soil experienced a more dramatic drop, with CBR falling from 14.02% to 8.61%, a 38.6% reduction. At the highest contamination level, neither soil met the typical minimum subgrade CBR requirement for pavement construction. A similar result and findings were observed by Rasheed et al., (2014). Their results showed that there was a decrease in the shear strength of the contaminated soil. The CBR value was seen to be decreasing from 3.7% to 2.2% as the percentage of kerosene contaminant increased from 0 to 7.5%, while a decrease to 1.8 as the percentage of gasoil contamination was increased to 7.5%.

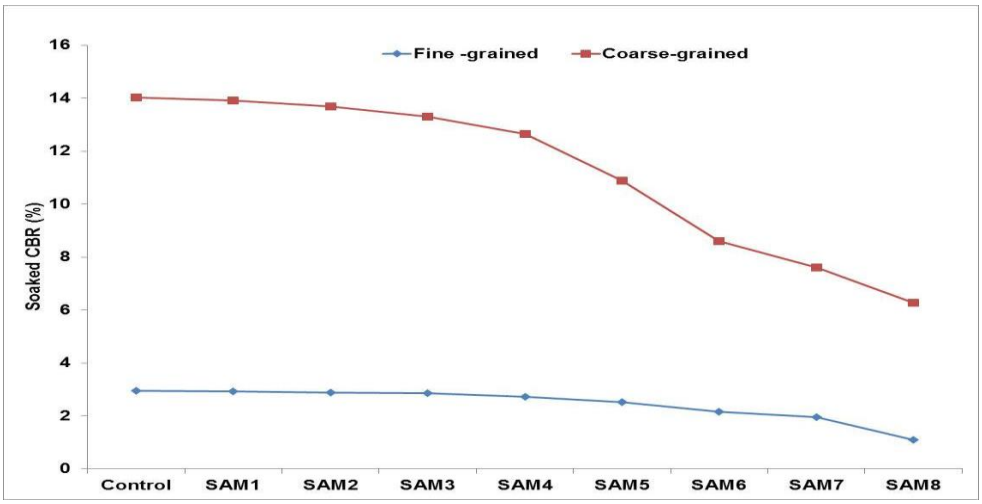

Figure 2: Soaked CBR Values of Contaminated Fine- and Coarse-Grained Soils

3.6 Soil Permeability

The permeability test results are summarised in Table 8. The fine-grained soil exhibited a consistent decrease in hydraulic conductivity with increasing contamination, falling from 2.26×10^{-8} m/s (control) to as low as 3.07×10^{-9} m/s at SAM 8, a reduction of over 86%. The coarse-grained soil also showed a steady decline in permeability, decreasing from 1.08×10^{-4} m/s to 7.31×10^{-5} m/s, representing a 32.3% reduction. The decrease was statistically significant in both soils, with the magnitude of change being more pronounced in the fine-grained soil despite its already low baseline permeability. The oil contamination induced a reduction in permeability of the samples. This is in line with the findings of Ayininuola et al., (2015). Also Khamehchiyan et al., (2007) obtained similar result in their study of the effect of crude oil on geotechnical properties of coastal soils. Similar results were equally obtained in Rahman, Umar and Ahmad (2010), and Sharma (2014).

Table 8: Permeability Values of Contaminated Soil Samples (Mean ± SD)

Factor	Fine-grained k (m/s)	Coarse-grained k (m/s)
Control	2.26E-08 ± 2.65E-10	1.08E-04 ± 4.04E-06
SAM 1 (2%)	2.19E-08 ± 2.52E-10	9.97E-05 ± 3.21E-07
SAM 2 (4%)	1.84E-08 ± 8.89E-10	9.41E-05 ± 4.36E-07
SAM 3 (6%)	1.23E-08 ± 4.51E-10	9.08E-05 ± 6.08E-07
SAM 4 (8%)	1.05E-08 ± 2.65E-10	8.94E-05 ± 8.62E-07
SAM 5 (10%)	9.53E-09 ± 2.52E-10	8.70E-05 ± 7.02E-07
SAM 6 (12%)	8.40E-09 ± 3.00E-10	8.30E-05 ± 9.64E-07
SAM 7 (14%)	7.20E-09 ± 3.00E-10	7.94E-05 ± 7.02E-07
SAM 8 (16%)	3.07E-09 ± 3.51E-10	7.31E-05 ± 7.81E-07

IV. Discussion

This study evaluated the combined impact of diesel and waste engine oil, a more realistic contamination scenario than single-product studies, on the geotechnical behavior of two contrasting soil types. The results confirm the overarching hypothesis that a mixture of petroleum hydrocarbons profoundly degrades soil quality, with the degree of alteration being a function of soil type and contaminant concentration.

The unexpected initial increase in liquid limit (LL) and plastic limit (PL) in fine-grained soil at low contamination levels (2-4%), before a sharp decline, represents a key finding. While a decrease in Atterberg limits is a commonly reported consequence of oil contamination (Khamehchiyan et al., 2007; Tse & Eshiemomo, 2016), the initial increase observed here contradicts that general trend but aligns with the findings of Kermani and Ebadi (2012) and Akinwumi et al. (2014). This phenomenon can be attributed to the mixed nature of the contaminant. At low concentrations, the lighter diesel fractions may initially penetrate and expand the interlayer space of clay minerals, but this weak interaction is later overwhelmed as heavier, more viscous engine oil components progressively coat the clay particles. This coating creates a hydrophobic barrier that displaces the water film (the diffuse double layer), ultimately reducing the soil's affinity for water and causing the LL and PL to drop (Rajabi & Sharifipour, 2018). In coarse-grained soil, the emergence of apparent plasticity is likely a pseudo-effect from the viscous binder of the waste oil coating sand particles and trapping fine materials, rather than a true electro-chemical change in plasticity.

The compaction results, showing a consistent decrease in MDD and an increase in OMC with higher contamination, agree with broad findings in the literature (Kermani & Ebadi, 2012; Salimnezhad et al., 2021). The decrease in MDD is due to the lower specific gravity of the hydrocarbons compared to soil solids, and the lubricating effect of the oil, which allows particles to slide past each other more easily under compactive effort. However, this same lubrication prevents effective mechanical interlocking and rigid packing, explaining the reduced density. The increase in OMC suggests that water is less effective at lubricating the particles for compaction, as non-polar hydrocarbons already occupy binding sites on particle surfaces and interfere with the surface tension mechanisms that normally facilitate moisture-density relationships.

The analysis of shear strength revealed a critical shift in the load-resisting mechanism of fine-grained soil. The decline in friction angle by 44.7% was accompanied by an initial increase in cohesion, a novel observation for this specific contaminant mixture. This is likely attributable to the capillary action and surface tension of the viscous waste engine oil, which would create menisci between particles, generating an apparent cohesion (Mohammadi et al., 2016). As contamination increased beyond 2%, this cohesion declined as the contaminant film thickened and began to physically push particles apart, disrupting the electrochemical bonds that underpin the soil's true cohesion (Obeta & Eze-Uzomaka, 2013; Oyegbile & Ayininuola, 2013). This result has critical theoretical implications; it challenges the simple application of the Mohr-Coulomb failure criterion without careful consideration of the pore fluid's viscous properties. For coarse-grained soil, the loss of the angle of internal friction stemmed purely from the physical lubrication of particle contacts, leading to a 32.7% reduction in internal friction.

The severe decline in soaked CBR is a direct measure of the loss of structural competency for pavement design. The 38.6% reduction in the CBR of coarse-grained soil, from a marginal subbase quality to a very poor subgrade, is particularly alarming and consistent with the findings of Ayininuola and Bajomo (2023). This can be explained by the combined effect of pore-clogging by viscous oils during soaking and the lubricated state of particle contacts, which allows for easier penetration of the CBR plunger. The paradox of decreased permeability in both soils, even as the clay's soil structure weakened, can be explained by the physical blockage of pore throats by the viscous, immiscible hydrocarbon droplets (George et al., 2014; Ostovar et al., 2020). This

reduction in drainage capacity could lead to significant pore-water pressure buildup under undrained loading, creating a dual hazard of high compressibility and potential for sudden loss of stability.

A primary limitation of this study is its short-term nature; the 28-day acclimatization period cannot fully simulate the long-term effects of aging, biodegradation, and chemical weathering that occur over years in a natural spill site. These processes could further alter soil properties or, conversely, lead to some natural recovery as volatile components evaporate (Al-Sanad et al., 1995; Youdeowei, 2008). Furthermore, the specific mineralogy of the clay, which strongly influences its interaction with hydrocarbons, was not analysed. While the results are directly applicable to the soils tested, their generalization requires caution, as different clay mineralogies (e.g., kaolinite vs. montmorillonite) would likely respond differently.

V. Conclusion

This study evaluated the combined effect of diesel and waste engine oil contamination on the geotechnical properties of fine-grained and coarse-grained soils, addressing the critical knowledge gap regarding mixed hydrocarbon pollution. The findings conclusively demonstrate that the co-occurrence of these petroleum products synergistically degrades soil engineering properties to a degree that renders both soil types unsuitable for direct construction use without prior stabilisation.

Contamination caused a concentration-dependent shift in Atterberg limits, with the liquid limit of fine-grained soil initially rising from 43.67% to 48.67% at 4% contamination before declining sharply to 26.67% at 16%, reflecting a transition from diesel-induced clay expansion to heavy oil coating that suppressed water affinity. Compaction efficiency was universally compromised, with maximum dry density falling by 16.9% (1.36 to 1.13 g/cm³) and 13.5% (1.78 to 1.54 g/cm³) in fine and coarse soils respectively, while optimum moisture content increased correspondingly. The angle of internal friction collapsed by 44.7% in fine-grained soil (25.33° to 14.00°) and 32.7% in coarse-grained soil (33.67° to 22.67°), while fine-grained soil exhibited a transient increase in apparent cohesion to 16.15 kN/m² at 2% contamination before declining, indicating a fragile, viscosity-dependent strength mechanism. Soaked CBR values fell severely, by 26.5% (2.94% to 2.16%) in fine soil and 38.6% (14.02% to 8.61%) in coarse soil, with the latter failing to meet subgrade requirements. Permeability decreased substantially in both soils, by over 86% in fine-grained soil, due to pore clogging by viscous hydrocarbons.

The broader significance of this work lies in demonstrating that site assessments based on single-contaminant exposure may be non-conservative when mixed wastes are present. Remediation prior to construction is therefore an essential engineering requirement, not merely an environmental precaution. Future research should investigate the long-term aging effects on these mixed-contaminant soils and evaluate the effectiveness of cementitious and pozzolanic stabilisation techniques for restoring their geotechnical integrity.

References

1. Ahmadi, M., Ebadi, T., & Maknoon, R. (2021). Effects of crude oil contamination on geotechnical properties of sand–kaolinite mixtures. Engineering Geology, 283, 106021. https://doi.org/10.1016/j.enggeo.2021.106021
2. Akinwumi, I.I., Diwa, D., and Obianigwe, N. (2014). Effects of crude oil contamination On the index properties, strength and permeability of lateritic clay. Int. journal of Applied Science and Engineering Research, 3(4), 816-824.
3. Akpokodje, O. I., Juwah, H. O., & Uguru, H. (2022). Impacts of petroleum spills on geotechnical properties of soils: A review. Journal of Engineering Innovations and Applications, 1(1), 1–6.
4. Al-Sanad, H. A., & Ismael, N. F. (1997). Aging effects on oil contaminated Kuwaiti sand. Journal of Geotechnical and Geoenvironmental Engineering, 123(3), 290–293.
5. Al-Sanad, H. A., Eid, W. K., & Ismael, N. F. (1995). Geotechnical properties of oil-contaminated Kuwaiti sand. Journal of Geotechnical Engineering, 121(5), 407–412.
6. Araz, S., Hossein, S., Ali, A.S. (2021). Effects of oil contamination and bioremediation on geotechnical properties of highly plastic clayey soil. Journal of Rock Mechanics and Geotechnical Engineering, 13(3), 653 - 670.

7. ASTM D1883-16. (2016). Standard test method for California Bearing Ratio (CBR) of laboratory-compacted soils. ASTM International. https://doi.org/10.1520/D1883-16
8. ASTM D3080-11. (2011). Standard test method for direct shear test of soils under consolidated drained conditions. ASTM International. https://doi.org/10.1520/D3080-11
9. ASTM D422-63(2007)e2. (2007). Standard test method for particle-size analysis of soils. ASTM International. https://doi.org/10.1520/D0422-63R07E02
10. ASTM D4318-17e1. (2017). Standard test methods for liquid limit, plastic limit, and plasticity index of soils. ASTM International. https://doi.org/10.1520/D4318-17E01
11. ASTM D5084-16a. (2016). Standard test methods for measurement of hydraulic conductivity of saturated porous materials using a flexible wall permeameter. ASTM International. https://doi.org/10.1520/D5084-16A
12. ASTM D698-12(2021). (2021). *Standard test methods for laboratory compaction characteristics of soil using standard effort (12,400 ft-lbf/ft3 (600 kN-m/m3))*. ASTM International. https://doi.org/10.1520/D0698-12R21
13. ASTM D720/D720M-15. (2015). Standard test methods for free swelling index of soils. ASTM International. https://doi.org/10.1520/D0720_D0720M-15
14. ASTM D854-14. (2014). Standard test methods for specific gravity of soil solids by water pycnometer. ASTM International. https://doi.org/10.1520/D0854-14
15. Ayininuola, G. M., & Bajomo, O. S. (2023). Suitability of crude oil-contaminated laterite as foundation base for roads and buildings. LAUTECH Journal of Civil and Environmental Studies, 11(1).
16. Ayininuola, G. M. & Kwashima, O. F. (2015). Effect of Diesel Oil Contamination on Soil Natural Recharge of Groundwater. 2nd International Conference on Geological and Civil Engineering, IPCBEE vol. 80 (2015) © (2015) IACSIT Press, Singapore.
17. Budhu, M. (2011). Soil mechanics and foundations (3rd ed.). John Wiley & Sons.
18. Das, B. M. (2010). Principles of geotechnical engineering (7th ed.). Cengage Learning.
19. George, S., Aswathy, E. A., Sabu, B., Krishnaprabha, N. P., & George, M. (2014). Study on geotechnical properties of diesel oil contaminated soil. International Journal of Civil and Structural Engineering Research, 2(2), 113–117.
20. Habib-ur-Rehman, Sahel N. A. and Tayyeb, A. (2017). Geotechnical Behavior of Oil-Contaminated Fine Grained Soils. ejge paper 2007 -0720, 1 - 12.
21. Ibrahim, A. U., Bello, A., & Nuhu, M. (2020). Environmental impact of used engine oil dumping in some selected motor parks in Kaduna Metropolis, Nigeria. Science World Journal, 15(1), 84–88.
22. Ijimdiya, T. S. (2013). The effects of oil contamination on the consolidation properties of lateritic soil. Development and Applications of Oceanic Engineering, 2(2), 53–59.

23. Kadafa, A. Y. (2012). Oil exploration and spillage in the Niger Delta of Nigeria. Civil and Environmental Research, 2(3), 38–49.

24. Kermani, M., & Ebadi, T. (2012). The effect of oil contamination on the geotechnical properties of fine-grained soils. Soil and Sediment Contamination: An International Journal, 21(5), 655–671.

25. Khamehchiyan, M., Charkhabi, A. H., & Tajik, M. (2007). Effects of crude oil contamination on geotechnical properties of clayey and sandy soils. Engineering Geology, 89(3–4), 220–229.

26. Mohammadi, A. H., Ebadi, T., Ahmadi, M., & Aliasghar, A. (2016). Shear strength behavior of crude oil contaminated sand-concrete interface. Civil Engineering Journal, 2(8), 362–371.

27. Nachum, S. (2025). Soil water potential in geosciences: An overview. Geosciences, 15(4), 123. https://doi.org/10.3390/geosciences15040123

28. Nwachukwu, A. N., Okoro, B. C., Osuagwu, J. C., Nwakwasi, N. L., & Onyechere, I. C. (2020). Index and compaction properties of oil contaminated clay soils in Niger-Delta region of Nigeria. Saudi Journal of Engineering and Technology, 5(2), 81–85.

29. Obeta, I. N., & Eze-Uzomaka, O. J. (2013). Geotechnical properties of waste engine oil contaminated laterites. Nigerian Journal of Technology, 32(2), 203–210.

30. Oluremi, J. R., Adewuyi, A. P., & Sanni, A. A. (2017). Compaction characteristics of oil contaminated residual soil. Journal of Engineering Research, 22(2), 56–67.

31. Ostovar, M., Ghiassi, R., Mehdizadeh, M. J., & Shariatmadari, N. (2020). Effects of crude oil on geotechnical specification of sandy soils. Soil and Sediment Contamination: An International Journal, 30(1), 58–73.

32. Oyegbile, O. B., & Ayininuola, G. M. (2013). Laboratory studies on the influence of crude oil spillage on lateritic soil shear strength: A case study of Niger Delta area of Nigeria. Journal of Earth Sciences and Geotechnical Engineering, 3(2), 73–83.

33. Rahman, Z. A., Hamzah, U., Taha, M. R., Ithnain, N. S., & Ahmad, N. (2010). Influence of oil contamination on geotechnical properties of basaltic residual soil. American Journal of Applied Sciences, 7(7), 954–961.

34. Rahman, Z.A, Umar, H. and Ahmad, N. (2010). Geotechnical characteristics of oil contaminated granite and mete sedimentary soils. Asian journal of Applied science, 3 (237-249).

35. Rajabi, H., & Sharifipour, M. (2018). Geotechnical properties of hydrocarbon-contaminated soils: a comprehensive review. Bulletin of Engineering Geology and the Environment, 78(5), 3685–3717.

36. Rasheed, Z. N Ahmed F. R. & Jassim, H. M. (2014). Effect of crude oil products on the geotechnical properties of soil. WIT Transactions on Ecology and The Environment, Vol 186, © WIT Press

37. Salimnezhad, A., Soltani-Jigheh, H., & Soorki, A. A. (2021). Effects of oil contamination and bioremediation on geotechnical properties of highly plastic clayey soil. Journal of Rock Mechanics and Geotechnical Engineering, 13(3), 653–670.

38. Sharma, R.K. (2014). Effect of Diesel pollution on sub-Grade and permeability characteristics of fly Ash-Sand composite. Proceedings of the Clute Institute International Academic Conference, Munich, Germany, 2014, pp 451-461.

39. Tamassoki, S., Daud, N. N. N., Wang, S., & Roshan, M. J. (2023). CBR of stabilized and reinforced residual soils using experimental, numerical, and machine-learning approaches. Transportation Geotechnics, 42, 101080. https://doi.org/10.1016/j.trgeo.2023.101080

40. Tse, A. C., & Eshiemomo, A. U. (2016). Geotechnical properties of soils in a crude oil impacted site in the Niger Delta, Nigeria. IOSR Journal of Applied Geology and Geophysics, 4(2), 69–76.

41. Youdeowei, P. O. (2008). The effect of crude oil pollution and subsequent fire on the engineering properties of soils in the Niger Delta. Bulletin of Engineering Geology and the Environment, 67(1), 119–121.